Spin isovector responses in finite nuclei.

Spin isovector responses in finite nuclei

W. M. Alberico,[a] A. De Pace,[b] and A. Molinari[a]
[a]*Istituto di Fisica Teorica dell'Università di Torino, Torino, Italy*
[b]*Scuola di Specializzazione in Fisica Nucleare, Torino, Italy*
and Istituto Nazionale di Fisica Nucleare, Sezione di Torino, Torino, Italy
(Received 7 November 1984)

We present a unified investigation of the spin-isospin responses of a finite nucleus in both the spin-transverse ($\sigma\times\mathbf{q}$) and spin-longitudinal ($\sigma\cdot\mathbf{q}$) channels, utilizing the formalism of the polarization propagator, $\Pi\mu\nu$. The independent particle transverse response (evaluated in a harmonic oscillator basis) fails to reproduce the recent data from deep inelastic (e,e′) scattering, thus pointing to the existence of collective effects. As a preliminary step toward the solution of the random-phase-approximation equations for $\Pi\mu\nu$, we explore in detail the mixed-coupling propagator, which may produce significant differences between the collective response of infinite nuclear matter and the one of a finite system.

I. INTRODUCTION

The nuclear response function in the spin-isospin channel has been widely considered in the last few years. A substantial amount of theoretical and experimental work has been carried out to clarify its features, together with the nature of the spin-isospin force and the role played by pions and Δ isobars inside nuclei.

Recently it has been suggested[1] that the nuclear response, providing it is collective in character, should be markedly different, at least in some range of momentum transfers q, in the spin longitudinal ($\sigma\cdot\mathbf{q}$) channel as compared with the spin transverse one ($\sigma\times\mathbf{q}$).

The origin of the contrast lies in the attraction mediated by pions, which may overcome, for $q\approx 2\mu_\pi$, the well-established short range repulsion of the spin-isospin particle-hole force, thus producing some enhancement and softening in the longitudinal response. In the transverse one, instead, which cannot be directly coupled to the pion, the opposite occurs, namely a quenching and a hardening.

These results were obtained in infinite nuclear matter, in an RPA (random phase approximation) framework. A recent experimental search[2] has shown no evidence of this effect. It is conceivable that this outcome may also be associated with finite size effects;[3] indeed, in a confined system the presence of the surface mixes pionlike and rholike excitations and a reduction of the expected contrast could thus occur.

Therefore it is of relevance to explore the spin-isospin response in a finite nucleus. This we intend to do in the present and in a forthcoming paper, with the method of the polarization propagator. The latter can be generally defined as

$$\Pi_{\mu a,\nu b}(\mathbf{x}t,\mathbf{x}'t') = -\frac{i}{\hbar}\langle\Psi_0|\,T\{\tilde{j}_{H\mu a}(\mathbf{x}t)\tilde{j}^{\dagger}_{H\nu b}(\mathbf{x}'t')\}\,|\Psi_0\rangle\,, \tag{1.1}$$

where T is the time-ordered product,

$$\tilde{j}_{H\mu a}(\mathbf{x}t)=\hat{j}_{H\mu a}(\mathbf{x}t)-\langle\Psi_0|\,\hat{j}_{H\mu a}(\mathbf{x}t)\,|\Psi_0\rangle \tag{1.2}$$

is the current deviation operator in Heisenberg representation, $|\Psi_0\rangle$ is the exact ground state of the nuclear Hamiltonian, and μ,ν and a,b are vector and isospin indices, respectively.

In the above, $\hat{j}_{H\mu a}$ is expressed in terms of field operators as follows:

$$\hat{j}_{H\mu a}(\mathbf{x}t)=\int d\mathbf{y}\,\hat{\psi}^{\dagger}_H(\mathbf{y},t)j_{\mu a}(\mathbf{x}-\mathbf{y})\hat{\psi}_H(\mathbf{y},t) = \sum_{\alpha,\beta}\langle\alpha\,|\,j_{\mu a}(\mathbf{x})\,|\,\beta\rangle\hat{a}^{\dagger}_{H\alpha}(t)\hat{a}_{H\beta}(t)\,, \tag{1.3}$$

where

$$\langle\alpha\,|\,j_{\mu a}(\mathbf{x})\,|\,\beta\rangle=\int d\mathbf{y}\,\psi^{\dagger}_{\alpha}(\mathbf{y})j_{\mu a}(\mathbf{x}-\mathbf{y})\psi_{\beta}(\mathbf{y}) \tag{1.4}$$

are the first quantized matrix elements of the current between the single particle states $\psi_\alpha(\mathbf{y})$, and $\hat{a}^{\dagger},\hat{a}$, the anticommuting fermion operators.

With the aim of calculating and comparing the spin longitudinal and spin transverse responses, we introduce the following spin-isospin four-current:

(i) $\mu=m$ $(=1,2,3)$,

$$j_{ma}(\mathbf{x}-\mathbf{y})=\frac{\tau_a}{2}\frac{i}{(2\pi)^3}\int d\mathbf{q}(\sigma\times\mathbf{q})_m e^{-i\mathbf{q}\cdot(\mathbf{x}-\mathbf{y})}\,; \tag{1.5a}$$

(ii) $\mu=0$,

$$\rho_a(\mathbf{x}-\mathbf{y})\equiv j_{0a}(\mathbf{x}-\mathbf{y}) = \tau_a\frac{i}{(2\pi)^3}\int d\mathbf{q}(\sigma\cdot\mathbf{q})e^{-i\mathbf{q}\cdot(\mathbf{x}-\mathbf{y})}\,; \tag{1.5b}$$

τ_a $(a=x,y,z)$ being the Pauli isospin matrices of the nucleon.

In order to evaluate the nuclear response to an external probe of definite momentum and energy, it is more convenient to work in momentum space where the Fourier transform of (1.1) can be written as

$$\Pi_{\mu a,\nu b}(\mathbf{q},\mathbf{q}';\omega) = \sum_{n\neq 0}\left[\frac{\langle\Psi_0|\hat{j}_{\mu a}(\mathbf{q})|\Psi_n\rangle\langle\Psi_n|\hat{j}_{\nu b}(-\mathbf{q}')|\Psi_0\rangle}{\hbar\omega-(E_n-E_0)+i\eta} - \frac{\langle\Psi_0|\hat{j}_{\nu b}(-\mathbf{q}')|\Psi_n\rangle\langle\Psi_n|\hat{j}_{\mu a}(\mathbf{q})|\Psi_0\rangle}{\hbar\omega+(E_n-E_0)-i\eta}\right], \tag{1.6}$$

where

$$\hat{H}|\Psi_n\rangle = E_n|\Psi_n\rangle\ , \tag{1.7}$$

$\hat{H}$ being the full nuclear Hamiltonian.

In (1.6) the current operators are now in the Schrödinger picture and the Fourier transform of the matrix elements in (1.3) can be easily carried out for the four-current (1.5):

$$\langle\alpha|j_{ma}(\mathbf{q})|\beta\rangle = \frac{i}{2}\int d\mathbf{y}\,\psi_\alpha^\dagger(\mathbf{y})\tau_a(\boldsymbol{\sigma}\times\mathbf{q})_m e^{i\mathbf{q}\cdot\mathbf{y}}\psi_\beta(\mathbf{y})\ , \tag{1.8a}$$

$$\langle\alpha|\rho_a(\mathbf{q})|\beta\rangle \equiv \langle\alpha|j_{0a}(\mathbf{q})|\beta\rangle = i\int \mathbf{dy}\,\psi_\alpha^\dagger(\mathbf{y})\tau_a(\boldsymbol{\sigma}\cdot\mathbf{q})e^{i\mathbf{q}\cdot\mathbf{y}}\psi_\beta(\mathbf{y})\ . \tag{1.8b}$$

The above relations obviously imply

$$\hat{j}^\dagger_{\nu b}(\mathbf{q}') = \hat{j}_{\nu b}(-\mathbf{q}') \tag{1.9}$$

which was utilized in (1.6).

The latter can then be conveniently rewritten in the form

$$\Pi_{\mu a,\nu b}(\mathbf{q},\mathbf{q}';\omega) = \sum_{n\neq 0}\left[\frac{\langle\Psi_0|\hat{j}_{\mu a}(\mathbf{q})|\Psi_n\rangle\langle\Psi_n|\hat{j}_{\nu b}(-\mathbf{q}')|\Psi_0\rangle}{\hbar\omega-(E_n-E_0)+i\eta} - \frac{\text{c.c.}(\mathbf{q}\to-\mathbf{q},\mathbf{q}'\to-\mathbf{q}')}{\hbar\omega+(E_n-E_0)-i\eta}\right]. \tag{1.10}$$

An expression alternative to (1.6) and useful in writing down the RPA integral equations reads[4]

$$\Pi_{\mu a,\nu b}(\mathbf{q},\mathbf{q}';\omega) = \frac{1}{\hbar}\sum_{\alpha\beta\gamma\delta}\langle\alpha|j_{\mu a}(\mathbf{q})|\beta\rangle\langle\gamma|j_{\nu b}(-\mathbf{q}')|\delta\rangle\Lambda_{\beta\alpha,\gamma\delta}(\omega)\ , \tag{1.11}$$

with

$$\Lambda_{\beta\alpha,\gamma\delta}(\omega) = \hbar\sum_{n\neq 0}\left[\frac{\langle\Psi_0|\hat{a}^\dagger_\alpha\hat{a}_\beta|\Psi_n\rangle\langle\Psi_n|\hat{a}^\dagger_\gamma\hat{a}_\delta|\Psi_0\rangle}{\hbar\omega-(E_n-E_0)+i\eta} - \frac{\langle\Psi_0|\hat{a}^\dagger_\gamma\hat{a}_\delta|\Psi_n\rangle\langle\Psi_n|\hat{a}^\dagger_\alpha\hat{a}_\beta|\Psi_0\rangle}{\hbar\omega+(E_n-E_0)-i\eta}\right]. \tag{1.12}$$

In Sec. II we shall evaluate the zeroth-order approximation to the polarization propagator (pure shell model) and in Sec. III we test its space components on the spin transverse nuclear response of ^{40}Ca, recently separated out in Saclay.[5]

The poor performance of the shell model in interpreting the data asks for a collective approach to the nuclear response. Accordingly in Sec. IV we discuss the RPA equations (neglecting antisymmetrization) for both the space (spin transverse) and the time (spin longitudinal) components of $\Pi_{\mu a,\nu b}(\mathbf{q},\mathbf{q}';\omega)$. These equations will be solved in a forthcoming paper. Here we limit ourselves to explore in detail, in Sec. V, the features of the density-current polarization propagator, which is responsible for the coupling between the spin-transverse and spin-longitudinal channels.

II. INDEPENDENT PARTICLE POLARIZATION PROPAGATOR

We now evaluate (1.6) in the independent particle approximation, which amounts to replacing $|\Psi_n\rangle$ with Slater determinants of single-particle wave functions, to be denoted by $|\phi_n\rangle$. For convenience we use the harmonic oscillator (HO) basis for spin $\frac{1}{2}$, isospin $\frac{1}{2}$ particles:

$$\psi_\alpha^{\text{HO}}(\mathbf{r}) = \varphi_{n_\alpha l_\alpha m_\alpha}(\mathbf{r})\chi_{s_\alpha}\eta_{t_\alpha}\ , \tag{2.1}$$

where

$$\varphi_{n_\alpha l_\alpha m_\alpha}(\mathbf{r}) = R_{n_\alpha l_\alpha}(r)Y_{l_\alpha m_\alpha}(\hat{r}) \tag{2.2}$$

corresponds to the eigenvalues $\epsilon_{n_\alpha l_\alpha}$.

Let us now consider separately the time, space, and mixed components of the polarization propagator (1.6), which we shall refer to as density-density, current-current, and current-density (or density-current), respectively.

A. Density-density polarization propagator

According to (1.10), it is defined as

$$\Pi^0_{0a,0b}(\mathbf{q},\mathbf{q}';\omega) \equiv \Pi^0_{a,b}(\mathbf{q},\mathbf{q}';\omega) = \sum_{n\neq 0}\left[\frac{\langle\phi_0|\hat{\rho}_a(\mathbf{q})|\phi_n\rangle\langle\phi_n|\hat{\rho}_b(-\mathbf{q}')|\phi_0\rangle}{\hbar\omega-(E^0_n-E^0_0)+i\eta} - \frac{\text{c.c.}(\mathbf{q}\to-\mathbf{q},\mathbf{q}'\to-\mathbf{q}')}{\hbar\omega+(E^0_n-E^0_0)-i\eta}\right], \tag{2.3}$$

where we have dropped, for convenience, the subscripts referring to the time components of j_μ.

We need, e.g., the matrix element

$$\langle \phi_n \mid \hat{\rho}_b(-\mathbf{q}') \mid \phi_0 \rangle = -i \sum_{\text{ph}} \langle \phi_n \mid \hat{a}^\dagger_{\text{p}} \hat{a}_{\text{h}} \mid \phi_0 \rangle \chi^\dagger_{s_{\text{p}}} (\boldsymbol{\sigma}\cdot\mathbf{q}') \chi_{s_{\text{h}}} \eta^\dagger_{t_{\text{p}}} \tau_b \eta_{t_{\text{h}}} \int d\mathbf{r}' e^{-i\mathbf{q}'\cdot\mathbf{r}'} \varphi^*_{n_{\text{p}} l_{\text{p}} m_{\text{p}}}(\mathbf{r}') \varphi_{n_{\text{h}} l_{\text{h}} m_{\text{h}}}(\mathbf{r}') \tag{2.4}$$

which we shall evaluate by coupling the particle and the hole to a definite angular momentum l, spin σ, and isospin τ. Moreover l and σ are coupled to a total angular momentum J. In the jj coupling scheme we get, after some algebra,

$$\langle \phi_n \mid \hat{\rho}_b(-\mathbf{q}') \mid \phi_0 \rangle = \sum_{\substack{JMl\sigma \\ \tau\tau_z}} \sum_{\substack{n_{\text{p}} l_{\text{p}} j_{\text{p}} \\ n_{\text{h}} l_{\text{h}} j_{\text{h}}}} \langle \phi_n \mid \text{ph};JM;\tau\tau_z \rangle \delta_{\sigma,1} \langle j_{\text{p}} j_{\text{h}};J \mid l\sigma;J \rangle (i)^{l+1} (-1)^{l_{\text{p}}} 4[\pi(2l_{\text{p}}+1)(2l_{\text{h}}+1)(2l+1)]^{1/2}$$
$$\times \begin{bmatrix} l & 1 & J \\ 0 & 0 & 0 \end{bmatrix} \begin{bmatrix} l_{\text{p}} & l_{\text{h}} & l \\ 0 & 0 & 0 \end{bmatrix} \mathscr{T}_{l n_{\text{p}} l_{\text{p}} n_{\text{h}} l_{\text{h}}}(q') Y^*_{JM}(\hat{\mathbf{q}}') \delta_{\tau,1} \Delta_{\tau_z,b} , \tag{2.5}$$

where

$$\Delta_{\tau_z,b} = \delta_{\tau_z,0}\delta_{b,z} - \delta_{\tau_z,1}(\delta_{b,x} - i\delta_{b,y})/\sqrt{2} + \delta_{\tau_z,-1}(\delta_{b,x} + i\delta_{b,y})/\sqrt{2} ,$$
$$\mathscr{T}_{l n_{\text{p}} l_{\text{p}} n_{\text{h}} l_{\text{h}}}(q) = q \int_0^\infty dr\, r^2 j_l(qr) R_{n_{\text{p}} l_{\text{p}}}(r) R_{n_{\text{h}} l_{\text{h}}}(r) , \tag{2.6}$$

and the symbol $\langle j_{\text{p}} j_{\text{h}};J \mid l\sigma;J \rangle$ is related to the $9j$ coefficients in the usual way:

$$\langle j_{\text{p}} j_{\text{h}};J \mid l\sigma;J \rangle = [(2j_{\text{p}}+1)(2j_{\text{h}}+1)(2l+1)(2\sigma+1)]^{1/2} \begin{Bmatrix} l_{\text{p}} & \frac{1}{2} & j_{\text{p}} \\ l_{\text{h}} & \frac{1}{2} & j_{\text{h}} \\ l & \sigma & J \end{Bmatrix} . \tag{2.7}$$

Let us now, following Toki and Weise,[6] define

$$a_{Jl} \equiv (J010 \mid l0) = (-1)^l \sqrt{2l+1} \begin{bmatrix} l & 1 & J \\ 0 & 0 & 0 \end{bmatrix} \tag{2.8}$$

and

$$Q^{Jl}_{\text{ph}}(q) = \langle j_{\text{p}} j_{\text{h}};J \mid l\sigma;J \rangle \delta_{\sigma,1} (-i)^{l+1} (-1)^{l_{\text{h}}} 4[\pi(2l_{\text{p}}+1)(2l_{\text{h}}+1)]^{1/2} \mathscr{T}_{l n_{\text{p}} l_{\text{p}} n_{\text{h}} l_{\text{h}}}(q) \begin{bmatrix} l_{\text{p}} & l_{\text{h}} & l \\ 0 & 0 & 0 \end{bmatrix} . \tag{2.9}$$

The expression (2.5) can then be recast as

$$\langle \phi_n \mid \hat{\rho}_b(-\mathbf{q}') \mid \phi_0 \rangle = \sum_{\substack{JM\tau\tau_z \\ l\sigma}} \sum_{\substack{n_{\text{p}} l_{\text{p}} j_{\text{p}} \\ n_{\text{h}} l_{\text{h}} j_{\text{h}}}} \langle \phi_n \mid \text{ph};JM;\tau\tau_z \rangle a_{Jl} Q^{Jl*}_{\text{ph}}(q') Y^*_{JM}(\hat{\mathbf{q}}') \delta_{\tau,1} \Delta_{\tau_z,b} . \tag{2.10}$$

Once (2.10) is inserted into (2.3) one finally gets

$$\Pi^0_{a,b}(\mathbf{q},\mathbf{q}';\omega) = \delta_{a,b} \sum_J \Pi^0_J(q,q';\omega) \frac{2J+1}{4\pi} P_J(\hat{\mathbf{q}}\cdot\hat{\mathbf{q}}') , \tag{2.11}$$

with

$$\Pi^0_J(q,q';\omega) = \sum_{ll'} a_{Jl} [\hat{\Pi}^0_J(q,q';\omega)]_{ll'} a_{Jl'} \tag{2.12}$$

and

$$[\hat{\Pi}^0_J(q,q';\omega)]_{ll'} = \sum_{\text{ph}} Q^{Jl}_{\text{ph}}(q) \left[\frac{1}{\hbar\omega - (\epsilon_{\text{p}} - \epsilon_{\text{h}}) + i\eta} - \frac{1}{\hbar\omega + (\epsilon_{\text{p}} - \epsilon_{\text{h}}) - i\eta} \right] Q^{Jl'*}_{\text{ph}}(q') \tag{2.13}$$

(note that ph is a shortcut for $n_{\text{p}} l_{\text{p}} j_{\text{p}}$, $n_{\text{h}} l_{\text{h}} j_{\text{h}}$).

It is interesting to note than when the spin-orbit coupling is disregarded in the single-particle energies, then the summation over $j_{\text{p}}, j_{\text{h}}$ is trivial and $\hat{\Pi}^0_J$ turns out to be both diagonal in l and J independent. Thus instead of (2.12) we shall have

$$\Pi^0_J(q,q';\omega) = \sum_l a^2_{Jl} \hat{\Pi}^0_l(q,q';\omega) , \tag{2.14}$$

with

$$\hat{\Pi}^0_l(q,q';\omega)=16\pi\sum_{\substack{n_p l_p\\ n_h l_h}}(2l_p+1)(2l_h+1)\begin{bmatrix} l_p & l_h & l\\ 0 & 0 & 0\end{bmatrix}^2\mathcal{I}_{ln_pl_pn_hl_h}(q)$$

$$\times\left[\frac{1}{\hbar\omega-(\epsilon_{n_pl_p}-\epsilon_{n_hl_h})+i\eta}-\frac{1}{\hbar\omega+(\epsilon_{n_pl_p}-\epsilon_{n_hl_h})-i\eta}\right]\mathcal{I}_{ln_pl_pn_hl_h}(q')\ . \tag{2.15}$$

The summation over J can now be carried out, yielding finally, "in lieu" of (2.11),

$$\Pi^0_{a,b}(\mathbf{q},\mathbf{q}';\omega)=\delta_{a,b}(\hat{\mathbf{q}}\cdot\hat{\mathbf{q}}')\sum_l\hat{\Pi}^0_l(q,q';\omega)\frac{(2l+1)}{4\pi}P_l(\hat{\mathbf{q}}\cdot\hat{\mathbf{q}}')\ , \tag{2.16}$$

with $\hat{\Pi}^0_l$ given now by (2.15).

B. Density-current polarization propagator

It reads

$$\Pi^0_{0a,nb}(\mathbf{q},\mathbf{q}';\omega)=\sum_{K\neq0}(-1)^n\left[\frac{\langle\phi_0|\hat{\rho}_a(\mathbf{q})|\phi_K\rangle\langle\phi_K|\hat{j}_{-nb}(-\mathbf{q}')|\phi_0\rangle}{\hbar\omega-(E^0_K-E^0_0)+i\eta}-\frac{(-1)^n\text{c.c.}(\mathbf{q}\to-\mathbf{q},\mathbf{q}'\to-\mathbf{q}',n\to-n)}{\hbar\omega+(E^0_K-E^0_0)-i\eta}\right], \tag{2.17}$$

where the vector indices of the current are now the spherical ones ($n=0,\pm1$). We notice here that, for the spherical components of the current, Eq. (1.9) becomes

$$\hat{j}^\dagger_{nb}(\mathbf{q})=(-1)^n\hat{j}_{-nb}(-\mathbf{q})\ .$$

The current matrix element turns out to be

$$\langle\phi_K|\hat{j}_{-nb}(-\mathbf{q}')|\phi_0\rangle=\sum_{\text{ph}}\langle\phi_K|\hat{a}^\dagger_p\hat{a}_h|\phi_0\rangle(-i)\chi^\dagger_{s_p}(\sigma\times\mathbf{q}')_{-n}\chi_{s_h}\tfrac{1}{2}\eta^\dagger_{t_p}\tau_b\eta_{t_h}\int d\mathbf{r}'e^{-i\mathbf{q}'\cdot\mathbf{r}'}\varphi^*_{n_pl_pm_p}(\mathbf{r}')\varphi_{n_hl_hm_h}(\mathbf{r}') \tag{2.18}$$

and, with the same notation of (2.5),

$$\langle\phi_K|\hat{j}_{-nb}(-\mathbf{q}')|\phi_0\rangle=-i\sum_{\substack{JMJ'M'\\ \tau\tau_z l\sigma}}\sum_{\text{ph}}\langle\phi_K|\text{ph};JM;\tau\tau_z\rangle\sqrt{3/2}[(2J+1)(2J'+1)]^{1/2}$$

$$\times\begin{bmatrix} J & J' & 1\\ M & -M' & n\end{bmatrix}\begin{Bmatrix} J & J' & 1\\ 1 & 1 & l\end{Bmatrix}(-1)^{J'+M}Y^*_{J'M'}(\hat{\mathbf{q}}')a_{J'l}Q^{Jl*}_{\text{ph}}(q')\delta_{\tau,1}\Delta_{\tau_z,b}\ . \tag{2.19}$$

Inserting now (2.19) and (2.10) into (2.17), one ends up with

$$\Pi^0_{0a,nb}(\mathbf{q},\mathbf{q}';\omega)=i\sqrt{3/2}\delta_{a,b}\sum_{JM}\overline{\Pi}^0_J(q,q';\omega)(-1)^{M+J+n+1}\begin{bmatrix} J & J & 1\\ M & -n-M & n\end{bmatrix}Y_{JM}(\hat{\mathbf{q}})Y^*_{J,M+n}(\hat{\mathbf{q}}')\ , \tag{2.20}$$

where

$$\overline{\Pi}^0_J(q,q';\omega)=\sum_{ll'}a_{Jl}[\hat{\Pi}^0_J(q,q';\omega)]_{ll'}b^J_{Jl'} \tag{2.21}$$

and $[\hat{\Pi}^0_J(q,q';\omega)]_{ll'}$ is given by (2.13). In (2.21)

$$b^{J_1}_{Jl}=[(2J+1)(2J_1+1)]^{1/2}a_{J_1l}\begin{Bmatrix} J & J_1 & 1\\ 1 & 1 & l\end{Bmatrix}\ . \tag{2.22}$$

In deriving (2.20) one should observe that the parity of $J+J'$ [cf. (2.19)] must be the same of $l+l'$ [cf. (2.10)], which is even [cf. (2.9)]. Then the triangular condition of the $3j$ symbol in Eq. (2.19) implies $J'=J$.

As in the previous instance, when the spin-orbit coupling is disregarded, Eq. (2.21) simplifies to

$$\overline{\Pi}^0_J(q,q';\omega)=\sum_l a_{Jl}\hat{\Pi}^0_l(q,q';\omega)b^J_{Jl}\ , \tag{2.23}$$

with $\hat{\Pi}^0_l$ given by (2.15).

Remarkably the elements of (2.20) diagonal in momentum space identically vanish, since

$$\sum_M (-1)^M \begin{bmatrix} J & J & 1 \\ M & -n & -M & n \end{bmatrix} Y_{JM}(\hat{\mathbf{q}}) Y^*_{J,n+M}(\hat{\mathbf{q}}) = 0 \ . \tag{2.24}$$

This will be the case in infinite nuclear matter, where all the polarization propagators conserve the momentum.

In conclusion, the following relation between the current-density and the density-current propagators holds

$$\Pi^0_{na,0b}(\mathbf{q},\mathbf{q}';\omega) = (-1)^n \Pi^0_{0b,-na}(\mathbf{q}',\mathbf{q};\omega) \ . \tag{2.25}$$

C. Current-current polarization propagator

It reads

$$\Pi^0_{ma,nb}(\mathbf{q},\mathbf{q}';\omega) = \sum_{K\neq 0} (-1)^n \left[\frac{\langle \phi_0 | \hat{j}_{ma}(\mathbf{q}) | \phi_K \rangle \langle \phi_K | \hat{j}_{-nb}(-\mathbf{q}') | \phi_0 \rangle}{\hbar\omega - (E^0_K - E^0_0) + i\eta} - \frac{\langle \phi_0 | \hat{j}_{-nb}(-\mathbf{q}') | \phi_K \rangle \langle \phi_K | \hat{j}_{ma}(\mathbf{q}) | \phi_0 \rangle}{\hbar\omega + (E^0_K - E^0_0) - i\eta} \right] . \tag{2.26}$$

The matrix elements needed for its calculation have been previously derived and one gets the following expression:

$$\Pi^0_{ma,nb}(\mathbf{q},\mathbf{q}';\omega) = \delta_{a,b}\tfrac{3}{2} \sum_{\substack{JJ_1J_2 \\ MM_1M_2}} (-1)^{m+n} \begin{bmatrix} J & J_1 & 1 \\ M & -M_1 & m \end{bmatrix} \begin{bmatrix} J & J_2 & 1 \\ M & -M_2 & n \end{bmatrix} Y_{J_1M_1}(\hat{\mathbf{q}}) Y^*_{J_2M_2}(\hat{\mathbf{q}}') \Pi^0_{J;J_1J_2}(q,q';\omega) \ , \tag{2.27}$$

with

$$\Pi^0_{J;J_1J_2}(q,q';\omega) = \sum_{ll'} b^{J_1}_{Jl} [\hat{\Pi}^0_J(q,q';\omega)]_{ll'} b^{J_2}_{Jl'} \ , \tag{2.28}$$

the $b^{J'}_{Jl}$ being given by (2.22) and $\hat{\Pi}^0_J(q,q';\omega)$ again by (2.13). Also in this instance, when the spin orbit is neglected, (2.28) reduces to

$$\Pi^0_{J;J_1J_2}(q,q';\omega) = \sum_l b^{J_1}_{Jl} \hat{\Pi}^0_l(q,q';\omega) b^{J_2}_{Jl} \tag{2.29}$$

with $\hat{\Pi}^0_l$ given by Eq. (2.15).

Furthermore, from Eq. (2.27) it is easy to prove the following property:

$$\Pi^0_{ma,nb}(\mathbf{q},\mathbf{q}';\omega) = (-1)^{m+n} \Pi^0_{-ma,-nb}(\mathbf{q}',\mathbf{q};\omega) \ . \tag{2.30}$$

The diagonal matrix elements of (2.26) can be cast into the form

$$\Pi^0_{ma,nb}(\mathbf{q},\mathbf{q};\omega) = \delta_{a,b}\tfrac{3}{2} \sum_{JJ'J_1J_2} (-1)^{J+n} \left[\frac{(2J_1+1)(2J_2+1)(2J'+1)}{4\pi} \right]^{1/2} \Pi^0_{J;J_1J_2}(q,q;\omega) \times \begin{bmatrix} 1 & 1 & J' \\ m & -n & n-m \end{bmatrix} \begin{bmatrix} J_1 & J_2 & J' \\ 0 & 0 & 0 \end{bmatrix} \begin{Bmatrix} 1 & 1 & J' \\ J_1 & J_2 & J \end{Bmatrix} Y^*_{J',n-m}(\hat{\mathbf{q}}) \tag{2.31}$$

which will be utilized in the following section. In particular, when the spin-orbit coupling is neglected in the single-particle levels, (2.31) can be simply rewritten as

$$\Pi^0_{ma,nb}(\mathbf{q},\mathbf{q};\omega) = \delta_{a,b}\tfrac{1}{2} \sum_l \frac{(2l+1)}{4\pi} \hat{\Pi}^0_l(q,q;\omega) \left[\tfrac{1}{3}\delta_{m,n} + (-1)^{1+m}\sqrt{2\pi/3}\, Y_{2,m-n}(\hat{\mathbf{q}}) \begin{bmatrix} 1 & 1 & 2 \\ m & -n & n-m \end{bmatrix} \right] . \tag{2.32}$$

III. THE NUCLEAR SINGLE-PARTICLE TRANSVERSE RESPONSE

The nuclear transverse magnetic response, separated out with deep inelastic (e,e') scattering at Bates[7] and Saclay,[5] is the natural testing ground of the theory developed in the previous paragraph. The nucleonic electromagnetic current, which enters into the $\Pi_{ma,nb}$ appropriate for the evaluation of the magnetic response, requires somewhat different isospin operators, namely $[\mu_0/e(\mu_p-\mu_n)]\tau_3$ should replace τ_a and τ_b (we neglect here the small isoscalar contribution); μ_0 is the nuclear Bohr magneton,

$\mu_p=2.79$ and $\mu_n=-1.91$.

The nuclear transverse response (or transverse structure function) is then customarily defined as

$$S_T(q,\omega)=-\frac{1}{\pi}\frac{\mu_0^2}{e^2}(\mu_p-\mu_n)^2 G_M^2(q_\lambda^2) \times\sum_{m,n}\left[\delta_{m,n}-(-1)^{n+m}\frac{1}{q^2}q_{-m}q_n\right] \times \mathrm{Im}\Pi_{m3,n3}(\mathbf{q},\mathbf{q};\omega)\ , \tag{3.1}$$

m,n being spherical indices; in the above formula $G_M^2(q_\lambda^2)$ is the usual electromagnetic γNN form factor,

$$G_M(q_\lambda^2)=\frac{1}{[1+(q^2-\omega^2/c^2)/(18.1\ \mathrm{fm}^{-2})]^2}\ . \tag{3.2}$$

Obviously the second term in the square brackets of the right-hand side (rhs) of (3.1) does not contribute since the currents in $\Pi_{m,n}$ are orthogonal to $\mathbf{q}$.

Assuming, furthermore, the direction of the momentum $\mathbf{q}$, transferred to the nuclear system, along the direction of the z axis, Eq. (3.1) simplifies to

$$S_T(q,\omega)=-\frac{\mu_0^2}{e^2}(\mu_p-\mu_n)^2\frac{2}{\pi}\mathrm{Im}\Pi_{1,1}(\mathbf{q},\mathbf{q};\omega)G_M^2(q_\lambda^2)\ , \tag{3.3}$$

where the isospin indices have been dropped and (2.30) has been utilized. (Clearly the response, being a scalar quantity, is frame independent.)

From (2.32) it follows now

$$\Pi^0_{1,1}(\mathbf{q},\mathbf{q};\omega)=\tfrac{1}{4}\sum_l\frac{(2l+1)}{4\pi}\hat{\Pi}^0_l(q,q;\omega) \tag{3.4}$$

which, inserted into (3.3) together with the definition (2.15) of $\hat{\Pi}^0_l(q,q;\omega)$ gives, for the single-particle transverse response,

$$S_T^0(q,\omega)=\frac{\hbar^2q^2}{m^2c^2}\frac{(\mu_p-\mu_n)^2}{2\hbar\omega_0}G_M^2(q_\lambda^2) \times\sum_{n_p l_p n_h l_h}\sum_l\delta[\Delta N-(N_p-N_h)](2l_p+1)(2l_h+1)(2l+1)\begin{bmatrix} l_p & l_h & l\\ 0 & 0 & 0\end{bmatrix}^2\left[\frac{1}{q}\mathscr{T}_{ln_pl_pn_hl_h}(q)\right]^2\ , \tag{3.5}$$

where $\Delta N=\hbar\omega/\hbar\omega_0$ and the single particle HO energies have been expressed, in the usual way, as

$$\epsilon_{nl}=(2n+l+\tfrac{3}{2})\hbar\omega_0=(N+\tfrac{3}{2})\hbar\omega_0\ .$$

The transverse magnetic response of ^{40}Ca, ^{48}Ca, and ^{56}Fe have been recently measured at Saclay with deep inelastic electron scattering;[5] to compare with our theory we choose the data on ^{40}Ca, which is a closed shell nucleus even in the absence of spin-orbit coupling. The response, formula (3.5), is shown in Figs. 1 and 2, together with the experimental data, at $q=330$ and 410 MeV/c. The response of infinite nuclear matter is also displayed, with

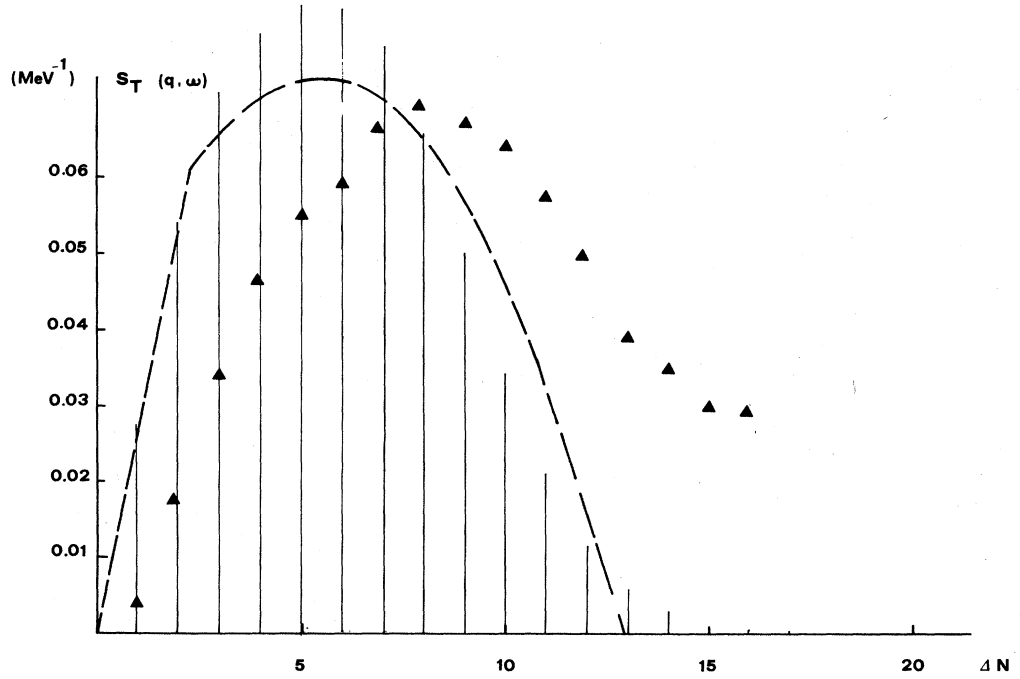

FIG. 1. The separated transverse magnetic response, Eq. (3.3), in ^{40}Ca at $q=330$ MeV/c as a function of $\hbar\omega=\Delta N\hbar\omega_0$. The experimental points (triangles) are taken from Ref. 5; the dashed line is the nuclear matter response, with $k_F=1.2$ fm^{-1}.

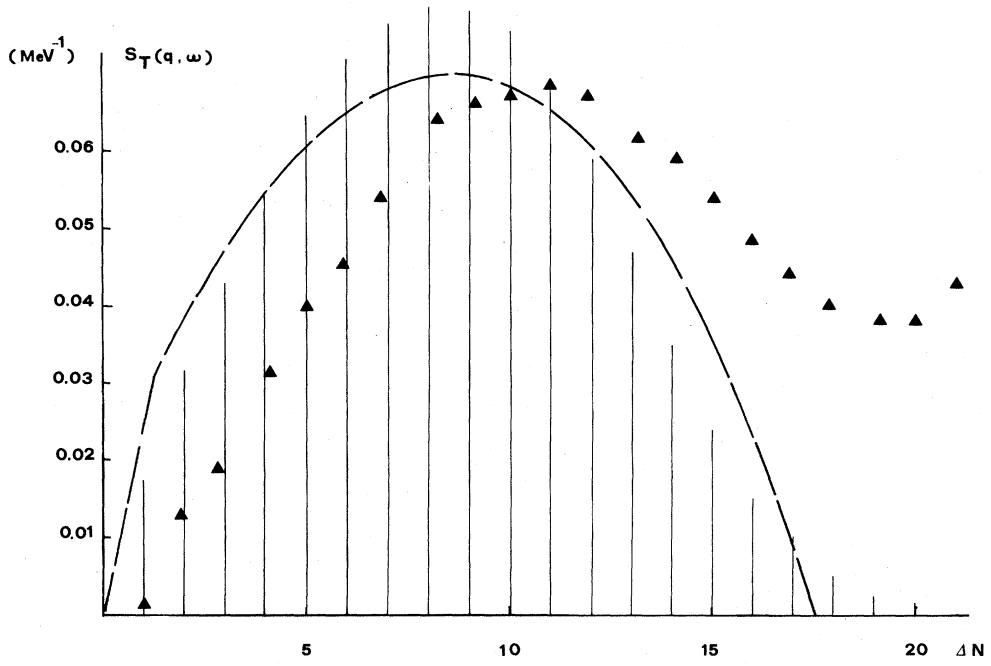

FIG. 2. The same as in Fig. 1, at $q=410$ MeV/c.

a Fermi wave number $k_F=1.2$ fm^{-1}.

These figures deserve a few comments:

(i) A systematic and substantial disagreement between theory and experiment shows up for all excitation energies: The theoretical response is enhanced at low frequencies and reduced at higher frequencies with respect to the data.

(ii) The responses of the nucleus (in the HO approximation) and of nuclear matter are rather close to each other, except for the features reflecting the confinement.[8] Moreover, in the present approach we have no free parameter at our disposal. Indeed, the oscillator parameter $\hbar\omega_0=11.02$ MeV is fixed by the rms radius of ^{40}Ca, whereas the nucleon mass and k_F can be utilized, in nuclear matter, to parametrize the effects of an average field.

(iii) As already pointed out in (i) and elsewhere,[1,9] the experimental transverse response displays some quenching and hardening with respect to the independent particle response. This behavior comes out naturally in an RPA theory for infinite nuclear matter, through the collective effects induced by the repulsive, short-ranged spin-isospin force, which indeed quench and harden the spin-transverse response.

Thus, we face the problem of evaluating the current-current polarization propagator in the frame of the RPA. In the next section we shall outline the theory; the corresponding numerical results will be given in a forthcoming paper.[10]

IV. THE RPA EQUATIONS FOR $\Pi_{\mu\nu}$

The random phase approximation to our polarization propagators can be most naturally derived utilizing Eq. (1.11), with $\Lambda^{\rm RPA}_{\beta\alpha,\gamma\delta}(\omega)$. The latter obeys the RPA equation[4]

$$\Lambda^{\rm RPA}_{\beta\alpha,\gamma\delta}(\omega)=\Lambda^{0}_{\beta\alpha,\gamma\delta}(\omega)+\frac{1}{\hbar}\times\sum_{\lambda\eta\sigma\rho}\Lambda^{0}_{\beta\alpha,\lambda\eta}(\omega)\langle\lambda\eta^{-1}\,|\,V\,|\,\sigma\rho^{-1}\rangle_D\times\Lambda^{\rm RPA}_{\sigma\rho,\gamma\delta}(\omega)\,, \tag{4.1}$$

where $\langle\lambda\eta^{-1}\,|\,V\,|\,\sigma\rho^{-1}\rangle_D$ is the direct particle-hole matrix element of the nucleon-nucleon interaction and

$$\Lambda^{0}_{\beta\alpha,\gamma\delta}(\omega)=\delta_{\alpha,\delta}\delta_{\beta,\gamma}\hbar\left[\frac{\theta(\gamma-F)\theta(F-\delta)}{\hbar\omega-(\epsilon^0_\gamma-\epsilon^0_\delta)+i\eta}-\frac{\theta(F-\gamma)\theta(\delta-F)}{\hbar\omega+(\epsilon^0_\delta-\epsilon^0_\gamma)-i\eta}\right], \tag{4.2}$$

F denoting the Fermi level.

Since we are exploring the spin-isospin particle-hole channel, the one-pion exchange, V_π, and the one-rho exchange, V_ρ, only will enter into play. To them it is customary to add a strongly repulsive, contact interaction, parametrized by the Landau-Migdal parameter g'. It accounts partially for exchange effects, which are neglected in (4.1).

With our previous definitions of the density-density, density-current, and current-current polarization propagators, we can write down three (formally) different integral RPA equations:

$$\Pi^{\mathrm{RPA}}_{ma,nb}(\mathbf{q},\mathbf{q}';\omega)=\Pi^{0}_{ma,nb}(\mathbf{q},\mathbf{q}';\omega)+\int\frac{d\mathbf{k}}{(2\pi)^3}\Pi^{0}_{ma,0c}(\mathbf{q},\mathbf{k};\omega)V^{L}_{cd}(k)\Pi^{\mathrm{RPA}}_{0d,nb}(\mathbf{k},\mathbf{q}';\omega)$$
$$+4\sum_{l=0,\pm1}\int\frac{d\mathbf{k}}{(2\pi)^3}\Pi^{0}_{ma,lc}(\mathbf{q},\mathbf{k};\omega)V^{T}_{cd}(k)\Pi^{\mathrm{RPA}}_{ld,nb}(\mathbf{k},\mathbf{q}';\omega)\ , \tag{4.3}$$

$$\Pi^{\mathrm{RPA}}_{0a,nb}(\mathbf{q},\mathbf{q}';\omega)=\Pi^{0}_{0a,nb}(\mathbf{q},\mathbf{q}';\omega)+\int\frac{d\mathbf{k}}{(2\pi)^3}\Pi^{0}_{0a,0c}(\mathbf{q},\mathbf{k};\omega)V^{L}_{cd}(k)\Pi^{\mathrm{RPA}}_{0d,nb}(\mathbf{k},\mathbf{q}';\omega)$$
$$+4\sum_{l=0,\pm1}\int\frac{d\mathbf{k}}{(2\pi)^3}\Pi^{0}_{0a,lc}(\mathbf{q},\mathbf{k};\omega)V^{T}_{cd}(k)\Pi^{\mathrm{RPA}}_{ld,nb}(\mathbf{k},\mathbf{q}';\omega)\ , \tag{4.4}$$

$$\Pi^{\mathrm{RPA}}_{0a,0b}(\mathbf{q},\mathbf{q}';\omega)=\Pi^{0}_{0a,0b}(\mathbf{q},\mathbf{q}';\omega)+\int\frac{d\mathbf{k}}{(2\pi)^3}\Pi^{0}_{0a,0c}(\mathbf{q},\mathbf{k};\omega)V^{L}_{cd}(k)\Pi^{\mathrm{RPA}}_{0d,0b}(\mathbf{k},\mathbf{q}';\omega)$$
$$+4\sum_{l=0,\pm1}\int\frac{d\mathbf{k}}{(2\pi)^3}\Pi^{0}_{0a,lc}(\mathbf{q},\mathbf{k};\omega)V^{T}_{cd}(k)\Pi^{\mathrm{RPA}}_{ld,0b}(\mathbf{k},\mathbf{q}';\omega)\ , \tag{4.5}$$

where

$$V^{L}_{ab}(k)=\Gamma^2_\pi(k^2)\frac{f^2_\pi}{\mu^2_\pi}\left[\frac{g'}{k^2}-\frac{1}{k^2+\mu^2_\pi}\right]\delta_{ab}\ , \tag{4.6a}$$

$$V^{T}_{ab}(k)=\left[\Gamma^2_\pi(k^2)\frac{f^2_\pi}{\mu^2_\pi}\frac{g'}{k^2}-\Gamma^2_\rho(k^2)\frac{f^2_\rho}{\mu^2_\rho}\frac{1}{k^2+\mu^2_\rho}\right]\delta_{ab}\ . \tag{4.6b}$$

In the above, $f^2_\pi/4\pi\hbar c=0.08$, $f^2_\rho/\mu^2_\rho=2.18$ (f^2_π/μ^2_π), and the usual monopole form factors have been included at the π (ρ) NN vertexes. The short-range repulsive force

$$V_{\mathrm{SR}}=\frac{f^2_\pi}{\mu^2_\pi}g'(\boldsymbol{\sigma}_1\cdot\boldsymbol{\sigma}_2)(\boldsymbol{\tau}_1\cdot\boldsymbol{\tau}_2) \tag{4.7}$$

has been incorporated into Eqs. (4.6) on the basis of the following identity:

$$(\boldsymbol{\sigma}_1\cdot\mathbf{k})(\boldsymbol{\sigma}_2\cdot\mathbf{k})+(\boldsymbol{\sigma}_1\times\mathbf{k})\cdot(\boldsymbol{\sigma}_2\times\mathbf{k})=k^2(\boldsymbol{\sigma}_1\cdot\boldsymbol{\sigma}_2)\ . \tag{4.8}$$

Notice that in Eqs. (4.3)—(4.5) the index 0 is referred to a "density," i.e., $(\boldsymbol{\sigma}\cdot\mathbf{q})$. We also remark that, since the p-h interaction is diagonal in the isospin indices, the following property holds:

$$\Pi^{\mathrm{RPA}}_{\mu a,\nu b}=\delta_{ab}\Pi^{\mathrm{RPA}}_{\mu,\nu} \tag{4.9}$$

and the isospin labels will be dropped hereafter.

Moreover, since the angular dependence of V^L and V^T [see Eqs. (4.6)] has been included into the polarization propagators, the latter display in RPA the same angular structure of the bare ones, namely,

$$\Pi^{\mathrm{RPA}}_{0,0}(\mathbf{q},\mathbf{q}';\omega)=\sum_{JM}\Pi^{\mathrm{RPA}}_{J}(q,q';\omega)Y_{JM}(\hat{\mathbf{q}})Y^{*}_{JM}(\hat{\mathbf{q}}')\ , \tag{4.10}$$

$$\Pi^{\mathrm{RPA}}_{0,n}(\mathbf{q},\mathbf{q}';\omega)=i\sqrt{3/2}\sum_{JM}\overline{\Pi}^{\mathrm{RPA}}_{J}(q,q';\omega)(-1)^{M+J+1+n}\begin{pmatrix}J & J & 1\\ M & -n-M & n\end{pmatrix}Y_{JM}(\hat{\mathbf{q}})Y^{*}_{JM+n}(\hat{\mathbf{q}}')\ , \tag{4.11}$$

$$\Pi^{\mathrm{RPA}}_{m,n}(\mathbf{q},\mathbf{q}';\omega)=\tfrac{3}{2}\sum_{\substack{JJ_1J_2\\ MM_1M_2}}(-1)^{m+n}\begin{pmatrix}J & J_1 & 1\\ M & -M_1 & m\end{pmatrix}\begin{pmatrix}J & J_2 & 1\\ M & -M_2 & n\end{pmatrix}Y_{J_1M_1}(\hat{\mathbf{q}})Y^{*}_{J_2M_2}(\hat{\mathbf{q}}')\Pi^{\mathrm{RPA}}_{J;J_1J_2}(q,q';\omega)\ , \tag{4.12}$$

where Π^{RPA}_J, $\overline{\Pi}^{\mathrm{RPA}}_J$, and $\Pi^{\mathrm{RPA}}_{J;J_1J_2}$ are given by (2.12), (2.21), and (2.28), respectively, providing that $\hat{\Pi}^{0}_J(q,q';\omega)$ is replaced by $\hat{\Pi}^{\mathrm{RPA}}_J(q,q';\omega)$ in all instances.

Then the three equations (4.3)—(4.5), after the angular variables have been integrated out, lead to a *unique* integral RPA equation for the matrix $\hat{\Pi}^{\mathrm{RPA}}_J$:

$$[\hat{\Pi}^{\mathrm{RPA}}_J(q,q';\omega)]_{ll'}=[\hat{\Pi}^{0}_J(q,q';\omega)]_{ll'}+\frac{1}{(2\pi)^3}\int_0^\infty dk\,k^2\sum_{l_1l_2}[\hat{\Pi}^{0}_J(q,k;\omega)]_{ll_1}[U_J(k)]_{l_1l_2}[\hat{\Pi}^{\mathrm{RPA}}_J(k,q';\omega)]_{l_2l'}\ , \tag{4.13}$$

with

$$[U_J(k)]_{l_1l_2}=a_{Jl_1}V^L(k)a_{Jl_2}+V^T(k)(\delta_{l_1l_2}-a_{Jl_1}a_{Jl_2})$$
$$=[V_\pi(k)-V_\rho(k)]a_{Jl_1}a_{Jl_2}+\delta_{l_1l_2}\left[V_\rho(k)+\Gamma^2_\pi(k^2)\frac{f^2_\pi}{\mu^2_\pi}\frac{g'}{k^2}\right]\ . \tag{4.14}$$

For fixed J, this is a 3×3 matrix since the factors a_{Jl} imply $l=J\pm1$.

One should also keep in mind that, in the spin-isospin channel, the nucleon can be virtually excited to a Δ isobar ($S=\frac{3}{2}$, $T=\frac{3}{2}$) and Δ-hole intermediate states should be included in the polarization propagator as well. This can be accomplished in a standard way (see, for instance, Ref. 6).

Methods for solving the RPA equations (4.3)—(4.5) and detailed results will be presented in a forthcoming paper.[10] However some physical insight can be gained already by the direct inspection of the equations themselves.

The relevant quantities are the density-density and current-current RPA polarization propagators, whose imaginary parts provide the spin-longitudinal and spin-transverse responses; with a common normalization, which allows for their direct comparison, they may be defined as follows:

$$R_L(q,\omega)=-\frac{1}{2\pi}\mathrm{Im}\Pi_{03,03}(\mathbf{q},\mathbf{q};\omega) \tag{4.15}$$

and

$$R_T(q,\omega)=-\frac{1}{\pi}\sum_{m,n}\delta_{m,n}\mathrm{Im}\Pi_{m3,n3}(\mathbf{q},\mathbf{q};\omega)\ , \tag{4.16}$$

the suffixes L and T meaning longitudinal and transverse, respectively.

In the independent particle approximation (4.15) and (4.16) obviously coincide, as it can be easily checked by inspecting the relative expressions of Sec. II. In the RPA theory the longitudinal and transverse spin-isospin responses have been found to be markedly different at intermediate momentum tranfers when calculated for an homogeneous system (infinite nuclear matter).[1]

The contrast between the two responses stems, in this case, from the distinct characteristics of the related particle-hole forces: the g' + rho exchange in the transverse channel is strongly repulsive, the g' + pion exchange in the longitudinal one is attractive. Indeed, in an infinite system the $(\boldsymbol{\sigma}\times\mathbf{q})$ and $(\boldsymbol{\sigma}\cdot\mathbf{q})$ vertexes get decoupled in the p-h polarization propagator.

On the contrary, in a finite nucleus pion and rho exchanges enter together in both the RPA equations for the density-density and the current-current polarization propagators [see Eqs. (4.3) and (4.5)]: This is why the problem of solving the two equations can be reduced to the solution of Eq. (4.13) alone, where the full spin-isospin p-h force appears.

From these considerations one could expect that the finite size of the system might remove the contrast between the spin-longitudinal and spin-transverse RPA nuclear responses, since it leads to the same renormalization in both channels for each of the multipoles $\hat{\Pi}_J$. However, the latter enter with different weights into the density-density and current-current polarization propagators [see (4.10) and (4.12)].

In fact, a deeper examination of Eqs. (4.3) and (4.5) shows that both the pion in (4.3) and the rho in (4.5) enter the RPA equation for the quantity which has the "opposite" coupling through the density-current (or the current-density) polarization propagator. Therefore this is the crucial quantity in determining the ultimate differences between the RPA responses of nuclear matter and finite nuclei (we recall that in the zeroth-order approximation they do not differ appreciably).

We shall discuss in detail the density-current polarization propagator in Sec. V. Still, it can be observed here that in the case it is negligible with respect to the density-density and current-current polarization propagators, the second term in the rhs of Eq. (4.3) and the third one in the rhs of Eq. (4.5) can be disregarded. In such a condition the two equations not only would decouple, but become substantially different, since the p-h force contains either the pion or the rho exchanges as in the infinite nuclear matter.

V. THE MIXING BETWEEN THE TRANSVERSE AND THE LONGITUDINAL CHANNELS

As stressed before, the mixing between pionlike and rholike excitations occurs, in the RPA frame, through the density-current polarization propagator. Previous studies have already focused the attention on this mixing. In particular Delorme *et al.*[11,12] have investigated the form factor of the 15.1 MeV, $J^\pi=1^+$ state of ^{12}C with the aim of elucidating, in an RPA scheme, the pionic influence on the $M1$ transition.

More recently, Cohen[13] has further analyzed this problem, finding again a substantial contribution of the pion in the transverse channel, whereas the influence of the rho in the pionic channel appears to be weaker (because of the large rho mass) and somewhat model dependent.

In this section we explore, both in momentum and coordinate space, the density-current polarization propagator which, being a three-vector, is frame dependent and in general is a function of seven variables. We start our analysis in momentum space, choosing a frame with the z axis pointing in the $\mathbf{q}$ direction and with the vector $\mathbf{q}'$ lying in the (x,z) plane. Then $\Pi^0_{0,n}$ will depend only upon four variables and Eq. (2.20) is easily seen to become (isospin indexes are dropped)

$$\Pi^0_{0,n}(\mathbf{q},\mathbf{q}';\omega)=i\sqrt{3/8}\sum_J(-1)^{J+1+n}\sqrt{(2J+1)}\times\begin{bmatrix}J & J & 1\\ 0 & -n & n\end{bmatrix}Y^*_{Jn}(\hat{\mathbf{q}}\cdot\hat{\mathbf{q}}',0)\times\overline{\Pi}^0_J(q,q';\omega) \tag{5.1}$$

which can be further simplified, when the spin-orbit coupling is neglected, as follows

$$\Pi^0_{0,n}(\mathbf{q},\mathbf{q}';\omega)=\delta_{n,\pm1}\frac{i}{2\sqrt{2}}\sqrt{1-(\hat{\mathbf{q}}\cdot\hat{\mathbf{q}}')^2}\times\sum_l\frac{(2l+1)}{4\pi}P_l(\hat{\mathbf{q}}\cdot\hat{\mathbf{q}}')\hat{\Pi}^0_l(q,q';\omega)\ . \quad (5.2)$$

The above is a well-suited expression for the comparison with the density-density propagator (2.16). Indeed the ratio between these two quantities turns out immediately to be given by

$$\frac{-i\Pi^0_{0,n}(\mathbf{q},\mathbf{q}';\omega)}{\Pi^0_{0,0}(\mathbf{q},\mathbf{q}';\omega)}=\frac{\sqrt{1-(\hat{\mathbf{q}}\cdot\hat{\mathbf{q}}')^2}}{2\sqrt{2}(\hat{\mathbf{q}}\cdot\hat{\mathbf{q}}')}\ , \quad (5.3)$$

remarkably independent upon $|\mathbf{q}|,|\mathbf{q}'|$ and the energy.

For completeness we also quote the expression of the current-current propagator in the same reference frame

$$\Pi^0_{m,n}(\mathbf{q},\mathbf{q}';\omega)=(-1)^{m+n\frac{3}{2}}\sum_{J,J_1,J_2}\left[\frac{2J_1+1}{4\pi}\right]^{1/2}Y^*_{J_2,n-m}(\hat{\mathbf{q}}\cdot\hat{\mathbf{q}}',0)\begin{bmatrix}J & 1 & J_1\\ m & -m & 0\end{bmatrix}\begin{bmatrix}J & 1 & J_2\\ m & -n & n-m\end{bmatrix}\Pi^0_{J;J_1J_2}(q,q';\omega) \quad (5.4)$$

or, when the spin-orbit coupling is disregarded,

$$\Pi^0_{m,n}(\mathbf{q},\mathbf{q}';\omega)=\sqrt{3\pi}\begin{bmatrix}1 & 1 & 1\\ m & -m & 0\end{bmatrix}\begin{bmatrix}1 & 1 & 1\\ m-n & n & -m\end{bmatrix}\times Y_{1,m-n}(\hat{\mathbf{q}}\cdot\hat{\mathbf{q}}',0)\times\sum_l\frac{(2l+1)}{4\pi}P_l(\hat{\mathbf{q}}\cdot\hat{\mathbf{q}}')\hat{\Pi}^0_l(q,q';\omega)\ . \quad (5.5)$$

When $m=n$ the above expression is simply related to the density-density propagator:

$$\Pi^0_{m,m}(\mathbf{q},\mathbf{q}';\omega)=\tfrac{1}{4}(\hat{\mathbf{q}}\cdot\hat{\mathbf{q}}')\sum_l\frac{(2l+1)}{4\pi}P_l(\hat{\mathbf{q}}\cdot\hat{\mathbf{q}}')\hat{\Pi}^0_l(q,q';\omega)\ ,$$
$$=\tfrac{1}{4}\Pi^0_{0,0}(\mathbf{q},\mathbf{q}';\omega)\ , \quad (5.6)$$

whereas for $m=\pm1$, $n=0$ it is related to the density-current propagator

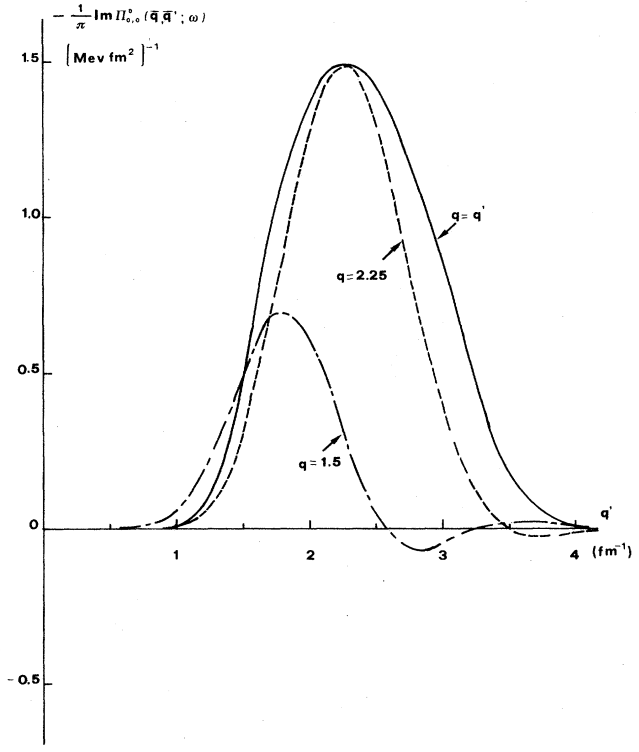

FIG. 3. The imaginary part of $\Pi^0_{0,0}(\mathbf{q},\mathbf{q}';\omega)$ in ^{40}Ca for $\hbar\omega=8\hbar\omega_0$ and $\hat{\mathbf{q}}\cdot\hat{\mathbf{q}}'=1$ as a function of q'. The continuous line represents the case $q=q'$, the dot-dashed line corresponds to $q=1.5$ fm^{-1}, and the dashed line to $q=2.25$ fm^{-1}.

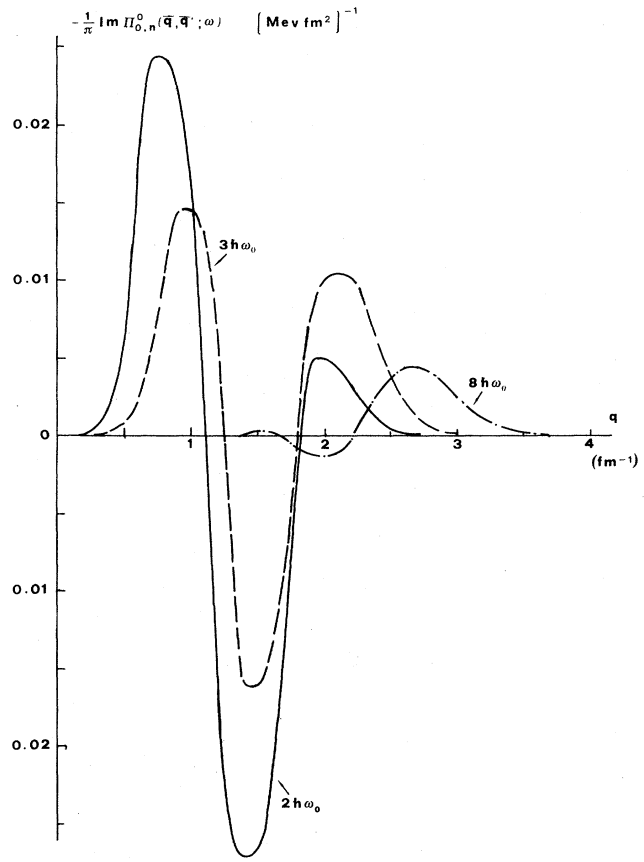

FIG. 4. The imaginary part of $\Pi^0_{0,n}(\mathbf{q},\mathbf{q}';\omega)$ in ^{40}Ca as a function of $q=q'$, with $\hat{\mathbf{q}}\cdot\hat{\mathbf{q}}'=0.5$ at different energies.

$$\Pi^0_{m,0}(\mathbf{q},\mathbf{q}';\omega)=\frac{m}{4\sqrt{2}}\sqrt{1-(\hat{\mathbf{q}}\cdot\hat{\mathbf{q}}')^2}\times\sum_l\frac{(2l+1)}{4\pi}P_l(\hat{\mathbf{q}}\cdot\hat{\mathbf{q}}')\hat{\Pi}^0_l(q,q';\omega)$$

$$=-\frac{im}{2}\Pi^0_{0,1}(\mathbf{q},\mathbf{q}';\omega)\ . \tag{5.7}$$

These relations are useful in discussing the role of the density-current polarization propagator in the RPA equations (4.3) and (4.5) and, consequently, the mixing between pion and rho in the spin-transverse and spin-longitudinal RPA responses.

The basic point is that for parallel $\mathbf{q}$ and $\mathbf{q}'$ ($\hat{\mathbf{q}}\cdot\hat{\mathbf{q}}'=1$) the density-density propagator reaches its maximum values whereas $\Pi^0_{0,n}$ vanishes.

For the sake of illustration we display in Fig. 3 the imaginary part of $\Pi^0_{0,0}(\mathbf{q},\mathbf{q}';\omega)$ at fixed energy ($\hbar\omega=8\hbar\omega_0$) and for $\hat{\mathbf{q}}\cdot\hat{\mathbf{q}}'=1$. Together with the fully diagonal term ($\mathbf{q}=\mathbf{q}'$), two cases with $|\mathbf{q}|\neq|\mathbf{q}'|$ are also displayed.

The imaginary part of the density-current propagator is shown instead in Fig. 4, for three different energies, when the angle between $\mathbf{q}$ and $\mathbf{q}'$ is $\pi/3$. In this case the ratio (5.3) is 0.61 and therefore $\Pi^0_{0,n}$ and $\Pi^0_{0,0}$ are of the same order of magnitude. However the scale of Fig. 4 is smaller than the one of Fig. 3 by a factor of order 10^{-2}.

Another important feature which appears in Fig. 4 concerns the energy dependence of the density-current propagator. In fact, as the energy increases it drops down rather quickly (in contrast with the behavior of the diagonal term of $\Pi^0_{0,0}$).

As the angle between $\mathbf{q}$ and $\mathbf{q}'$ increases toward $\pi/2$ the ratio (5.3) grows and $\Pi^0_{0,n}$ becomes larger than $\Pi^0_{0,0}$ (for instance their ratio is 1.73 for $\hat{\mathbf{q}}\cdot\hat{\mathbf{q}}'=0.2$), but its absolute value rapidly decreases by orders of magnitude. This is illustrated in Fig. 5 where the results for $\hat{\mathbf{q}}\cdot\hat{\mathbf{q}}'=0.5$ and $\hat{\mathbf{q}}\cdot\hat{\mathbf{q}}'=0.2$ are compared.

From the above considerations we argue that the role of the pion (rho) in the renormalization of the transverse (longitudinal) responses, although not negligible should not modify the nuclear matter results by more than 20—30 %. We also expect a progressive decoupling of the two channels as the energy increases.

We address now the question "where," inside the nucleus, the coupling between pionlike and rholike excitations plays the most relevant role. For this purpose we have investigated the density-current polarization propagator in coordinate space,

$$\Pi^0_{0,n}(\mathbf{r},\mathbf{r}';\omega)=\int\frac{d\mathbf{q}}{(2\pi)^3}e^{-i\mathbf{q}\cdot\mathbf{r}}\int\frac{d\mathbf{q}'}{(2\pi)^3}e^{i\mathbf{q}'\cdot\mathbf{r}'}\times\Pi^0_{0,n}(\mathbf{q},\mathbf{q}';\omega) \tag{5.8}$$

with $\Pi^0_{0,n}(\mathbf{q},\mathbf{q}';\omega)$ given by (2.20). The angular integrations are straightforward and lead to

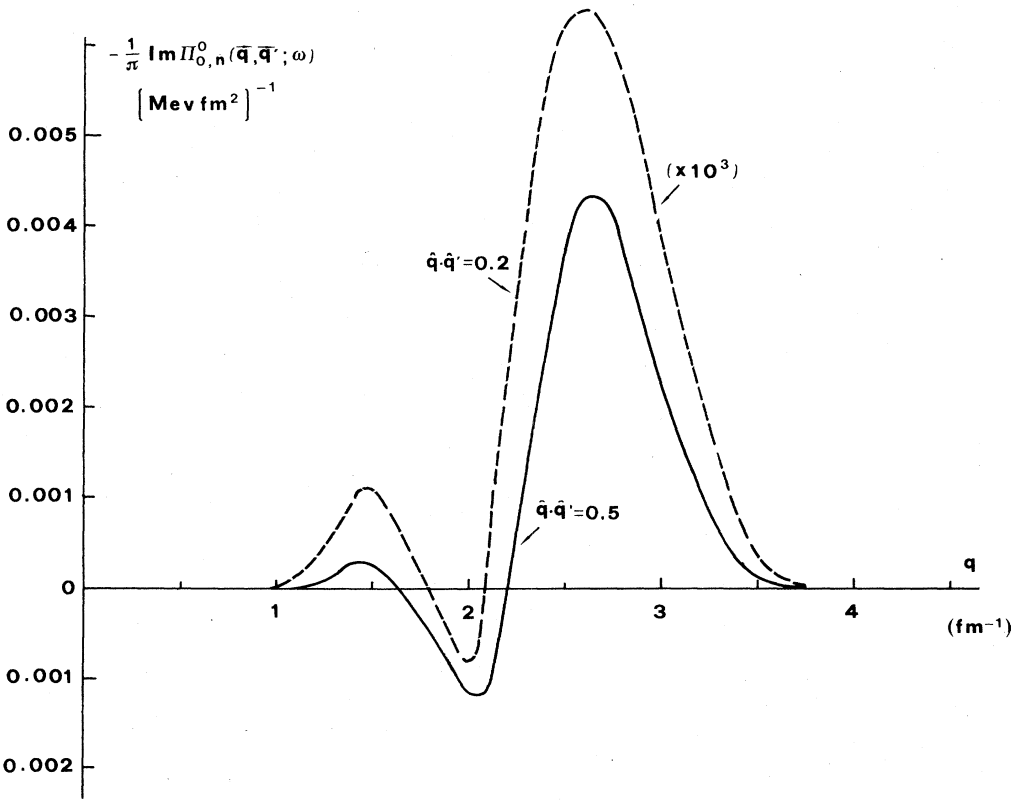

FIG. 5. The imaginary part of $\Pi^0_{0,n}(\mathbf{q},\mathbf{q}';\omega)$ in ^{40}Ca as a function of $q=q'$, with $\hbar\omega=8\hbar\omega_0$ at two different angles. The dashed curve has been multiplied by 10^3.

$$\Pi^0_{0,n}(\mathbf{r},\mathbf{r}';\omega)=i\sqrt{3/2}\sum_{JM}(-1)^{M+J+1+n}\begin{bmatrix}J & J & 1\\ M & -n-M & n\end{bmatrix}Y_{JM}(\hat{\mathbf{r}})Y^*_{J,M+n}(\hat{\mathbf{r}}')\sum_{ll'}a_{Jl}b^J_{Jl'}\sum_{\rm ph}F^{Jl}_{\rm ph}(r)\mathscr{D}_{\rm ph}(\omega)F^{Jl'*}_{\rm ph}(r')\ , \tag{5.9}$$

where

$$\mathscr{D}_{\rm ph}(\omega)=\frac{1}{\hbar\omega-(\epsilon_{\rm p}-\epsilon_{\rm h})+i\eta}-\frac{1}{\hbar\omega+(\epsilon_{\rm p}-\epsilon_{\rm h})-i\eta} \tag{5.10}$$

and

$$\begin{aligned}F^{Jl}_{\rm ph}(r)&=\frac{1}{2\pi^2}\int_0^\infty dq\,q^2j_J(qr)Q^{Jl}_{\rm ph}(q)\\&=\langle j_{\rm p}j_{\rm h};J\mid l\sigma;J\rangle\delta_{\sigma,1}(-i)^{l+1}(-1)^{l_{\rm h}}4[\pi(2l_{\rm p}+1)(2l_{\rm h}+1)]^{1/2}\begin{bmatrix}l_{\rm p} & l_{\rm h} & l\\ 0 & 0 & 0\end{bmatrix}\mathscr{A}^{Jl}_{\rm ph}(r)\ ,\end{aligned} \tag{5.11}$$

with

$$\mathscr{A}^{Jl}_{\rm ph}(r)=\frac{1}{2\pi^2}\int_0^\infty dq\,q^2j_J(qr)\mathscr{T}_{ln_{\rm p}l_{\rm p}n_{\rm h}l_{\rm h}}(q)\ . \tag{5.12}$$

The integral in (5.12) can be analytically calculated and the expression of $\mathscr{A}^{Jl}_{\rm ph}(r)$ is quoted in the Appendix. When the spin-orbit coupling is disregarded, (5.9) reduces to

$$\begin{aligned}\Pi^0_{0,n}(\mathbf{r},\mathbf{r}';\omega)=i\sqrt{3/2}\sum_{JM}(-1)^{J+M+1+n}&\begin{bmatrix}J & J & 1\\ M & -n-M & n\end{bmatrix}Y_{JM}(\hat{\mathbf{r}})Y^*_{J,M+n}(\hat{\mathbf{r}}')\\&\times\sum_l\sum_{\substack{n_{\rm p}l_{\rm p}\\ n_{\rm h}l_{\rm h}}}a_{Jl}b^J_{Jl}16\pi(2l_{\rm p}+1)(2l_{\rm h}+1)\begin{bmatrix}l_{\rm p} & l_{\rm h} & l\\ 0 & 0 & 0\end{bmatrix}^2\mathscr{A}^{Jl}_{\rm ph}(r)\mathscr{D}_{\rm ph}(\omega)\mathscr{A}^{Jl}_{\rm ph}(r')\ .\end{aligned} \tag{5.13}$$

Notice that the angular dependence of the density-current propagator in coordinate space is different from the one in momentum space, since now the J dependence is also associated with the radial variables, $|\mathbf{r}|$ and $|\mathbf{r}'|$ [compare Eq. (2.20)]. Still it remains true that for $\hat{\mathbf{r}}=\hat{\mathbf{r}}'$ (5.13) vanishes, as a consequence of (2.24).

We calculate $\Pi^0_{0,n}(\mathbf{r},\mathbf{r}';\omega)$ in a frame with the z axis parallel to $\mathbf{r}$ and the vector $\mathbf{r}'$ in the (x,z) plane. Then

$$\begin{aligned}\Pi^0_{0,n}(\mathbf{r},\mathbf{r}';\omega)=i\sqrt{3/2}\sum_J(-1)^{J+1+n}&\left[\frac{2J+1}{4\pi}\right]^{1/2}\begin{bmatrix}J & J & 1\\ 0 & -n & n\end{bmatrix}Y^*_{J,n}(\hat{\mathbf{r}}\cdot\hat{\mathbf{r}}',0)\\&\times\sum_l\sum_{\substack{n_{\rm p}l_{\rm p}\\ n_{\rm h}l_{\rm h}}}a_{Jl}b^J_{Jl}16\pi(2l_{\rm p}+1)(2l_{\rm h}+1)\begin{bmatrix}l_{\rm p} & l_{\rm h} & l\\ 0 & 0 & 0\end{bmatrix}^2\mathscr{A}^{Jl}_{\rm ph}(r)\mathscr{D}_{\rm ph}(\omega)\mathscr{A}^{Jl}_{\rm ph}(r')\ .\end{aligned} \tag{5.14}$$

The imaginary part of $-i\Pi^0_{0,n}(\mathbf{r},\mathbf{r}';\omega)$ is shown in Fig. 6 for two different angles ($\hat{\mathbf{r}}\cdot\hat{\mathbf{r}}'=0$ and $\hat{\mathbf{r}}\cdot\hat{\mathbf{r}}'=0.5$) and compared with the density-density propagator. In coordinate space the latter reads:

$$\Pi^0_{0,0}(\mathbf{r},\mathbf{r}';\omega)=\sum_J\frac{2J+1}{4\pi}P_J(\hat{\mathbf{r}}\cdot\hat{\mathbf{r}}')\sum_l a^2_{Jl}\sum_{\rm ph}16\pi(2l_{\rm p}+1)(2l_{\rm h}+1)\begin{bmatrix}l_{\rm p} & l_{\rm h} & l\\ 0 & 0 & 0\end{bmatrix}^2\mathscr{A}^{Jl}_{\rm ph}(r)\mathscr{D}_{\rm ph}(\omega)\mathscr{A}^{Jl}_{\rm ph}(r')\ . \tag{5.15}$$

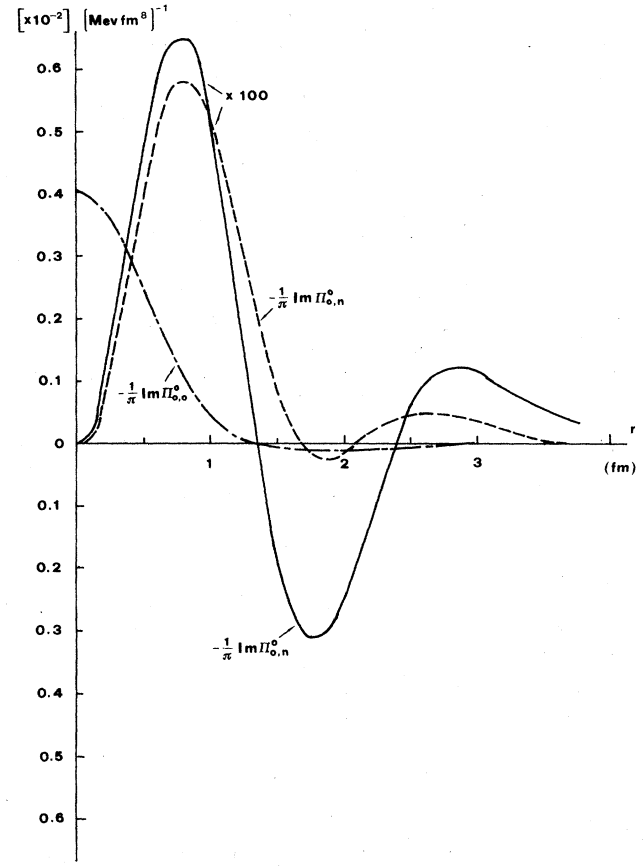

FIG. 6. Imaginary parts of $\Pi^0_{0,0}(\mathbf{r},\mathbf{r}';\omega)$ and $\Pi^0_{0,n}(\mathbf{r},\mathbf{r}';\omega)$ in ^{40}Ca as a function of $r=r'$. The dot-dashed line corresponds to $\Pi^0_{0,0}$ with $\hbar\omega=3\hbar\omega_0$ and $\hat{\mathbf{r}}\cdot\hat{\mathbf{r}}'=0.5$; the continuous and dashed lines correspond to $\Pi^0_{0,n}$ with $\hbar\omega=2\hbar\omega_0$ and $\hat{\mathbf{r}}\cdot\hat{\mathbf{r}}'=0$ or $\hat{\mathbf{r}}\cdot\hat{\mathbf{r}}'=0.5$, respectively. The latter curves have been multiplied by 10^2.

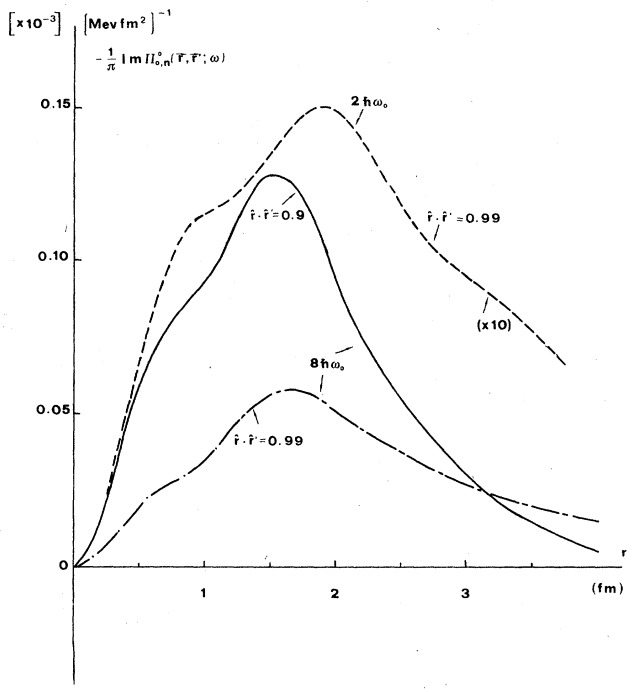

FIG. 7. The imaginary part of $\Pi^0_{0,n}(\mathbf{r},\mathbf{r}';\omega)$ in ^{40}Ca as a function of $r=r'$; the continuous line corresponds to $\hbar\omega=8\hbar\omega_0$ and $\hat{\mathbf{r}}\cdot\hat{\mathbf{r}}'=0.9$, the dot-dashed line to $\hbar\omega=8\hbar\omega_0$ and $\hat{\mathbf{r}}\cdot\hat{\mathbf{r}}'=0.99$, whereas the dashed line corresponds to $\hbar\omega=2\hbar\omega_0$ and $\hat{\mathbf{r}}\cdot\hat{\mathbf{r}}'=0.99$ (this curve is multiplied by a factor of 10).

The two propagators differ essentially for two reasons: (a) in general $\Pi^0_{0,n}$ is substantially smaller than $\Pi^0_{0,0}$; (b) at variance with $\Pi^0_{0,0}$, which is maximum in the center of the nucleus, the density-current propagator vanishes in the origin and displays its maximum at some finite distance, which depends upon the energy and the angle between $\mathbf{r}$ and $\mathbf{r}'$.

This is further illustrated in Fig. 7, where it is seen that for small energies and $\mathbf{r}'$ almost parallel to $\mathbf{r}$ the density-current propagator tends to peak at the nuclear surface, at least for small energies. A similar behavior is displayed by $\mathrm{Re}\,\Pi^0_{0,n}(\mathbf{r},\mathbf{r}';\omega)$.

It is conceivable that this peaking on the surface would be emphasized by densities which, unlike the harmonic oscillator one, flatten out inside the nucleus.

VI. CONCLUSIONS

In this paper we have explored the features of the spin-isospin polarization proagator. This quantity is viewed as a rank-two tensor, in a four-dimensional space, which allows for a unified treatment of the spin-longitudinal ($\sigma\cdot\mathbf{q}$) and spin-transverse ($\sigma\times\mathbf{q}$) couplings and of their interplay. Moreover, its imaginary part is directly linked to the longitudinal and transverse spin-isospin nuclear responses.

In the independent particle frame these responses coincide (but for trivial factors, linked to the nature of the probe one uses for their excitation). Furthermore, the shell model predictions are close to the nuclear matter ones, showing the irrelevance of the confinement for the single-particle response.

However, the spin-transverse nuclear response, as measured with deep inelastic electron scattering, hardly lends itself to an independent particle interpretation. Indeed, a marked disagreement between our harmonic oscillator calculation and the ^{40}Ca data is clearly apparent. One could argue that a more realistic Hartree-Fock basis is needed (among other failures, the HO basis does not reproduce correctly the nuclear central density).

Still, we believe that the observed discrepancy rather supports an interpretation of the experiment in terms of a *collective* response. In such a case, as it has been previously emphasized for infinite nuclear matter, the spin-longitudinal and spin-transverse nuclear responses should display a marked contrast, at least in the RPA frame. The question then arises whether the nuclear matter predictions still hold good in a finite nucleus.

A recent experiment of deep inelastic scattering of po-

larized protons, specifically devised for the direct comparison of the two spin responses, failed to bring to light the predicted contrast. Several items have been discussed in an attempt of intepreting this negative outcome. Here we stress the possibility that the mixing between $\sigma\cdot\mathbf{q}$ and $\sigma\times\mathbf{q}$, induced by the breaking of translational invariance, could substantially alter, in a finite nucleus, the behavior of the nuclear matter response, *particularly at low energies.*

This question can only be elucidated by directly solving the RPA equations, but an analysis of the density-current propagator can already shed some light on the problem. This quantity is highly nonlocal in momentum space and thus can only exist in a finite system.

We have explored its behavior both in momentum and in coordinate space: it turns out that $\Pi^0_{0,n}(\mathbf{q},\mathbf{q}';\omega)$ critically depends upon the angle between $\mathbf{q}$ and $\mathbf{q}'$; its ratio to the density-density (or to the current-current) propagators increases as $\hat{\mathbf{q}}\cdot\hat{\mathbf{q}}'$ goes from 1 to 0, but at the same time the magnitude of $\Pi^0_{0,n}$ decreases by orders of magnitude. Moreover, it tends to become smaller with increasing energy.

In coordinate space the diagonal terms of $\Pi^0_{0,n}$ still vanish; furthermore, $\Pi^0_{0,n}(\mathbf{r},\mathbf{r}';\omega)$ tends to zero when $|\mathbf{r}|$ (or $|\mathbf{r}'|$)$\rightarrow 0$, in contrast with $\Pi^0_{0,0}$ which, in the center of the nucleus, is maximum. The surface character of the density-current propagator would be even more pronounced in a Woods-Saxon basis.

We can conclude that the mixing of pionlike and rholike excitations is most important at low energy and is not linked to the *size* of the system, but rather to its *confinement.* It would be interesting to test our density-current propagator against the data of a (γ,π^0) experiment. The latter has recently been considered with renewed interest.[14]

We wish to thank Prof. M. Ericson and Dr. M. B. Johnson for interesting and stimulating discussions.

APPENDIX

In order to derive the expression for

$$\mathscr{A}^{Jl}_{\rm ph}(r)=\frac{1}{2\pi^2}\int_0^\infty dq\, q^2 j_J(qr)\mathscr{T}_{ln_{\rm p}l_{\rm p}n_{\rm h}l_{\rm h}}(q) \tag{A1}$$

let us recall the formula (see Ref. 8).

$$\begin{aligned}\mathscr{T}_{ln_{\rm p}l_{\rm p}n_{\rm h}l_{\rm h}}(q)=&\left[\frac{(2l_{\rm p}+2n_{\rm p}+1)!!(2l_{\rm h}+2n_{\rm h}+1)!!}{2^{n_{\rm p}+n_{\rm h}}n_{\rm p}!n_{\rm h}!}\right]^{1/2}\\ &\times\sum_{k=0}^{n_{\rm p}}\sum_{k'=0}^{n_{\rm h}}(-1)^{k+k'}\begin{bmatrix}n_{\rm p}\\ k\end{bmatrix}\begin{bmatrix}n_{\rm h}\\ k'\end{bmatrix}\frac{(l+l_{\rm p}+l_{\rm h}+2k+2k'+1)!!}{(2l_{\rm p}+2k+1)!!(2l_{\rm h}+2k'+1)!!}\\ &\times e^{-q^2/4\nu}\sum_{m=0}^{M}(-1)^m\begin{bmatrix}M\\ m\end{bmatrix}\frac{q^{2m+l+1}}{(2m+2l+1)!!}\frac{1}{(2\nu)^{m+l/2}}\end{aligned} \tag{A2}$$

which is valid in the HO basis. In (A2), $M=(l_{\rm p}+l_{\rm h}-l)/2+k+k'$ is an integer.

Therefore (A1) requires the calculation of

$$G(r)=\frac{1}{2\pi^2}\int_0^\infty dq\, e^{-q^2/4\nu}q^{2m+l+3}j_J(qr)\ , \tag{A3}$$

which turns out to be[8]

$$G(r)=\frac{1}{(2\pi)^{3/2}}(2m+l+J+2)!!(2\nu)^{m+2+(l+J)/2}r^J e^{-\nu r^2}\sum_{p=0}^{P}(-1)^p\begin{bmatrix}P\\ p\end{bmatrix}\frac{(2\nu r^2)^p}{(2J+2p+1)!!},\quad\left[P=\frac{l-J+1}{2}+m\right]. \tag{A4}$$

Inserting now (A2) into (A1) and utilizing (A4), one gets finally

$$\begin{aligned}\mathscr{A}^{Jl}_{\rm ph}(r)=&\frac{4\nu^2}{(2\pi)^{3/2}}(2\nu r^2)^{J/2}e^{-\nu r^2}\left[\frac{(2l_{\rm p}+2n_{\rm p}+1)!!(2l_{\rm h}+2n_{\rm h}+1)!!}{2^{n_{\rm p}+n_{\rm h}}n_{\rm p}!n_{\rm h}!}\right]^{1/2}\\ &\times\sum_{k=0}^{n_{\rm p}}\sum_{k'=0}^{n_{\rm h}}(-1)^{k+k'}\begin{bmatrix}n_{\rm p}\\ k\end{bmatrix}\begin{bmatrix}n_{\rm h}\\ k'\end{bmatrix}\frac{(l+l_{\rm p}+l_{\rm h}+2k+2k'+1)!!}{(2l_{\rm p}+2k+1)!!(2l_{\rm h}+2k'+1)!!}\\ &\times\sum_{m=0}^{M}(-1)^m\begin{bmatrix}M\\ m\end{bmatrix}\frac{(2m+l+J+2)!!}{(2m+2l+1)!!}\sum_{p=0}^{P}(-1)^p\begin{bmatrix}P\\ p\end{bmatrix}\frac{(2\nu r^2)^p}{(2J+2p+1)!!}\ .\end{aligned} \tag{A5}$$

[1]W. M. Alberico, M. Ericson, and A. Molinari, Nucl. Phys. **A379**, 429 (1982).
[2]T. A. Carey *et al.*, Phys. Rev. Lett. **53**, 144 (1984).
[3]W. M. Alberico, M. Ericson, and A. Molinari, Phys. Rev. C **30**, 1776 (1984).
[4]A. L. Fetter and J. D. Walecka, *Quantum Theory of Many-Particle Systems* (McGraw-Hill, New York, 1971).
[5]Z. E. Meziani *et al.*, Saclay Report No. 2163, 1984.
[6]H. Toki and W. Weise, Phys. Rev. Lett. **42**, 1034 (1979); Z. Phys. A **292**, 389 (1979).
[7]J. S. McCarthy, Nucl. Phys. A **335**, 27 (1980).
[8]W. M. Alberico, R. Cenni, V. R. Manfredi, and A. Molinari, Nuovo Cimento **40A**, 449 (1977).
[9]W. M. Alberico, M. Ericson, and A. Molinari, Ann. Phys. (N.Y.) **154**, 356 (1984).
[10]W. M. Alberico, A. De Pace, M. B. Johnson, and A. Molinari (unpublished).
[11]J. Delorme, M. Ericson, A. Figureau, and N. Giraud, Phys. Lett. **89B**, 327 (1980).
[12]J. Delorme, A. Figureau, and N. Giraud, Phys. Lett. **91B**, 328 (1980).
[13]Joseph Cohen, Phys. Rev. C **30**, 1238 (1984).
[14]D. R. Tieger *et al.*, Phys. Rev. Lett. **53**, 755 (1984).